Journal of Materials, Processing and Design (2024)
Clausius Scientific Press, Canada

DOI: 10.23977/jmpd.2024.080120
ISSN 2516-0923 Vol. 8 Num. 1

Numerical investigation of ballistic impact performance about ultra-high molecular weight polyethylene (UHMWPE) under high velocity impact

Jianhui Zhai, Yufen Zhao, Lu Hao, Bo Shang, Leilei Song[a,*], Changjian Qi

AECC Aegis Advanced Protective Technology Co., Ltd, Tianjin, 300300, China
[a]731416802@qq.com
[*]Corresponding author

Keywords: Ballistic impact performance, Finite element analysis, UHMWPE, Sub-laminate

Abstract: The ballistic impact performance of ultra-high molecular weight polyethylene (UHMWPE) cross-ply laminate under different fragment simulating projectiles (FSPs) is systematically investigated by commercial finite element software LS-DYNA. In order to simulate the composite laminate, sub-laminate model is used in three dimensional continuum scheme. Delamination model is characterized to simulate the bond between adjacent sub-laminates. The model is mainly validated by using the experimental result about a series of thicknesses of target composite plate under impacted by 7.5mm cubic FSP. We first study the impact process of simulated system under different impacted velocities and target thicknesses. We then use this information to investigate the energy absorption rate and ballistic performance index of target laminate in terms of a non-dimensional velocity or impacted velocity. Finally, we carry out the two sequence failure stages (local failure and bugling deformation) in numerical study and compare with others result.

1. Introduction

Ultra--high molecular weight polyethylene (UHMWPE) is widely used in armor protective applications due to its low mass density, high ultimate tensile strength, anti-corrosion, chemical resistance and excellent energy absorption capacity [1-4]. It is widely used in medical, aerospace, military and other important situations. Simultaneously, UHMWPE fiber has become the best choice in the field of protection due to its light weight, high strength, high stability and easy processing. Investigation of the dynamic response and damage mode of UHMWPE fiber and its composite panels under the combined effects of explosion shock wave and fragment penetration has practical significance for the further development of protective materials and protective engineering.

In order to deeply study the response and failure criteria of ultra-high molecular weight polyethylene under ballistic impact conditions, a large number of numerical simulations [5-11] were carried out. Zhang et al. [5] numerically investigated ballistic performance of UHMWPE laminate plates and UHMWPE was simulated through sub-laminate model. They found that the contact force between the projectile and the target plate had a correlation with the local small deformation and failure in thicker laminates. Then, Zhang et al. [6] numerically and experimentally explored

multilayered cross-ply UHMWPE. They found that multi-layered target could release the tensile stress of fiber on its back-side face and a significant pull-in effect is observed at the edges. These findings contributed to improved ballistic resistance and larger back-face deflection.

Nguyen et al. [10] studied the influence of target thickness on the ballistic performance of UHMWPE. They discovered that, for thicker UHMWPE laminate, the failure was divided into two sequence stages: in the first stage, shear plugging was dominate in local failure; in the second stage, bulging deformation (i.e. out-of plane deformation) played a significant role. Zhang et al. [12] performed a theoretical study of UHMWPE and found impact kinetic energy mainly dissipated by bulging deformation when the initial velocity increasing. The absorbed energy by local failure stage was linearly increased with initial velocity, while there was a suddenly drop at the ballistic limit velocity about the energy absorbed by bulging deformation stage. The failure of UHMWPE laminate was predominate by tensile modulus and failure strain of fibers.

In this research, LS-DYNA is used to simulate ballistic impact performance of cross-ply UHMWPE under impact of different FSPs. A detail description of numerical models is given in next section. Numerical implementation and material models such as Johnson-Cook material model, Mie-Grüneisen equation of state, sub-laminates composite model and delamination model. In this simulation, the model is mainly validated through 7.5 mm cubic FSP about a series of thicknesses of UHMWPE. Impact process analysis, energy absorption and penetration mechanism of target composite cross-ply plate are systematically investigated in numerical scheme.

2. Numerical models

2.1. Numerical implementation

The commercial finite element package LS-DYNA is used to simulate the ballistic impact performance of UHMWPE. In general, it is difficult to model delamination in laminated structure under continuum mechanics scheme. In order to accurately model ballistic response of UHMWPE cross-ply laminate, sub-laminate model is employed which has already been proved to be efficient [5,13,14]. Each sub-laminate is a combination of several cross-plies.

Eroding_single_Surf contact is applied between ballistic projectile and composite plate for modeling projectile erodes composite plate, and penetration between different plies is also avoided. An effective contact between projectile and UHMWPE sub-laminates is applied which is also known as soft constrain type 2 or pinball segment based contact.

There are two parts in UHMWPE impact model: fragment simulating projectile (FSP) and UHMWPE cross-ply laminate. There are two type of FSPs: one nose shape is truncate and another is cubic. The FSPs are made of ASTM 1045 steel. The FSPs are modeled by Johnson-Cook (J-C) constitutive model and J-C damage model. Mie-Grüneisen equation of state (EOS), which is suitable for solids under explosion and high pressure condition, is used together with J-C model, however it is not considered in UHMWPE laminate. The UHMWPE laminate is modeled by sub-laminate model and the connection of adjacent sub-laminates is realized by delamination model or tie-break model.

2.2. Material models and parameters

2.2.1. Johnson-Cook material model

The J-C yield surface or flow surface can be expressed as [15]

$$\sigma_{yield} = [A + B\varepsilon_p^n][1 + C\ln\dot{\varepsilon}_p^*][1 - T_H^m] \quad (1)$$

where ε_p, ε_p^* and T_H are equivalent plastic strain, strain rate ratio and non-dimensional or normalized temperature, respectively. ε_p^* is given by $\varepsilon_p^* = \dot{\varepsilon}_p / \dot{\varepsilon}_0$, where $\dot{\varepsilon}_p$ and $\dot{\varepsilon}_0$ are equivalent plastic strain rate and reference equivalent plastic strain rate, respectively. Normally, the reference equivalent plastic strain rate takes 1.0 s^{-1}. T_H is given as $(T - T_r)/(T_m - T_r)$, where T, T_r and T_m are current temperature, ambient temperature and melting temperature, respectively. *A*, *B*, *C*, *n* and *m* are material constants. The strain hardening, strain rate hardening and thermal softening are considered in J-C model.

J-C failure or damage model is derived from following cumulative damage criteria [16]

$$D = \sum \frac{\Delta \varepsilon_p}{\varepsilon_{failure}} \tag{2}$$

where $\Delta \varepsilon_p$ and $\varepsilon_{failure}$ are accumulated incremental effective plastic strain and current effective fracture strain, respectively. The effective fracture strain can be expressed as

$$\varepsilon_{failure} = [D_1 + D_2 \exp(D_3 \sigma^*)][1 + D_4 \ln \dot{\varepsilon}_p^*][1 + D_5 T_H^m] \tag{3}$$

where σ^*, $\dot{\varepsilon}_p^*$ and T_H are stress triaxiality, strain rate ratio and normalized temperature, respectively. D_1, D_2, D_3, D_4 and D_5 are material constants. The material constants of J-C constitutive model and J-C damage model are listed in Table 1.

Table 1: The J-C model material constants of ASTM 1045 steel [17].

$\rho(kg/m^3)$	E(GPa)	ν	A(MPa)	B(MPa)	n	C
7830	200	0.3	507	320	0.064	0.28
m	D_1	D_2	D_3	D_4	D_5	
1.06	0.1	0.76	1.57	0.005	-0.84	

Table 2: The Mie-Grüneisen parameters of ASTM 1045 steel [20].

$c(m/s)$	s_1	s_2	s_3	γ_0	a
5130	1.86	0.0	0.0	2.77	0

2.2.2. Mie-Grüneisen equation of state

The material state under impact loading can be described by the Mie-Grüneisen EOS. The Mie-Grüneisen is a theoretical model which is used for describing the thermodynamic properties of matter in a non-equilibrium state. The velocity of shockwave U is defined as a nonlinear relationship of the velocity of particle that just behind the shock [18]

$$U = c + s_1 u_p + s_2 \left(\frac{u_p}{U}\right) u_p + s_3 \left(\frac{u_p}{U}\right)^2 u_p \tag{4}$$

The pressure can be described in terms of specific volume and internal energy as [19]

$$P = \frac{\rho_0 c^2 \mu}{\left[1-(s_1-1)\mu - s_2\frac{\mu^2}{\mu+1} - s_3\frac{\mu^3}{(\mu+1)^2}\right]^2} + (\gamma_0 + a\mu)E, \mu > 0$$
$$P = \rho_0 c^2 \mu + (\gamma_0 + a\mu)E, \mu < 0 \tag{5}$$

where ρ_0, c and μ are reference density, the intercept of U-u_p curve and relative change of volume, respectively. s_1, s_2 and s_3 are material constants which can be obtained from U-u_p curve. Typically, s_2 and s_3 are zero for metals. γ_0, a and E are Grüneisen coefficient, first-order volume correction to γ_0 and internal energy, respectively. In our work, Mie-Grüneisen EOS is only considered for projectile and parameters are given in Table 2.

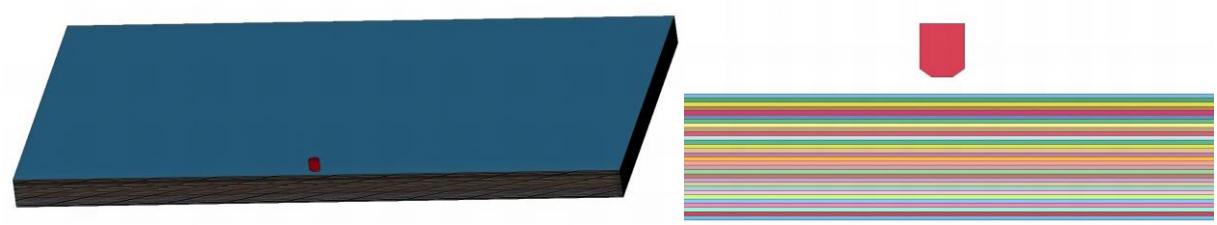

(a) (b)

Figure 1: Finite element model of UHMWPE under impacted by truncate FSP: (a) global, (b) local. The sub-laminates are given in different colors. For convenience, the finite element model under impacted by cubic FSP does not shown.

2.2.3. Sub-laminates composite model

Type #59 material model within LS-DYNA, which includes failure criteria, is suitable for three dimensional solid elements and is used to characterize the response of UHMWPE cross-ply laminate under dynamic impact frame. The stress-strain constitutive relationship of orthotropic can be described by the following formula:

$$\begin{Bmatrix} \varepsilon_a \\ \varepsilon_b \\ \varepsilon_c \\ \gamma_{bc} \\ \gamma_{ca} \\ \gamma_{ab} \end{Bmatrix} = \begin{bmatrix} \frac{1}{E_a} & -\frac{\nu_{ab}}{E_b} & -\frac{\nu_{ac}}{E_c} & 0 & 0 & 0 \\ -\frac{\nu_{ba}}{E_b} & \frac{1}{E_b} & -\frac{\nu_{bc}}{E_c} & 0 & 0 & 0 \\ -\frac{\nu_{ca}}{E_b} & -\frac{\nu_{cb}}{E_b} & \frac{1}{E_c} & 0 & 0 & 0 \\ 0 & 0 & 0 & G_{bc}^{-1} & 0 & 0 \\ 0 & 0 & 0 & 0 & G_{ca}^{-1} & 0 \\ 0 & 0 & 0 & 0 & 0 & G_{ab}^{-1} \end{bmatrix} \begin{Bmatrix} \sigma_a \\ \sigma_b \\ \sigma_c \\ \tau_{bc} \\ \tau_{ca} \\ \tau_{ab} \end{Bmatrix} \tag{6}$$

where ν, E and G are Poisson ration, Yang's modulus and shear modulus of UHMWPE sub-laminate, respectively. The subscripts a, b and c are denoted three orthogonal local material axes. a, b and c represent 0 °, 90 ° and through thickness direction of sub-laminate, respectively. Identical material properties are assumed along 0 ° and 90 ° directions since the UHMWPE laminate is cross-ply layup. Table 3 lists the material constants those are used during impact process of UHMWPE

sub-laminate.

Table 3: The material constants of UHMWPE sub-laminate [21, 22].

constants	value	constants	value
$\rho(kg/m^3)$	970	K_{fail} (GPa)	2.2
E_a, E_b (GPa)	30.7	ν_{ba}	0.008
E_c (GPa)	1.97	ν_{ca}, ν_{cb}	0.044
G_{ab} (GPa)	1.97	T_a, T_b, T_c (GPa)	3
G_{bc}, G_{ca} (GPa)	0.67	C_a, C_b, C_c (GPa)	2.5

Table 4: The material parameters of tie-break model.

NFLS	*SFLS*	*PARAM*
60[24]	80[25]	0.053[26]

2.2.4. Delamination model

There are several approaches in LS-DYNA for delamination modeling: cohesive zone element and tiebreak contact. Tiebreak contact has been proven to be a very effective algorithm for simulating delamination and is relatively simpler than the cohesive zone model [23].

Automatic_one_way_surface_to_surface_tiebreak with option 6 is adopted to model delamination between adjacent sub-laminates. This option is for use with solids and thick shells only. The one way contact tiebreak will only consider whether the slave surface nodes penetrate the master surface or not. The failure criteria of tiebreak contact is given by

$$\left(\frac{\sigma_n}{NFLS}\right)^2 + \left(\frac{\sigma_s}{SFLS}\right)^2 \geq 1 \tag{7}$$

where σ_n and σ_s are tensile normal and shear stresses, respectively. σ_n is taken as zero if the tensile normal stress is compressive. *NFLS*, *SFLS* and *PARAM* are normal, shear failure strengths and critical distance. Tiebreak is active for nodes which are initially in contact. The normal and shear stresses at the interface are scaled down as a function of the separation distance. When the separate distance reaches critical distance, the damage is fully developed and interface failure occurs. After failure, this contact option behaves as a surface to surface contact. The value of *NFLS*, *SFLS* and *PARAM* are listed in Table 4.

3. Validation

In order to balance calculation time and solution accuracy, we take half of the model as numerical model. The constructed numerical model of UHMWPE under impacted by FSP are shown in Fig. 1. The in-plane dimensions of the UHMWPE is 300mm×150mm in our work. Initial velocity boundary condition is applied to projectile. Fixed boundary conditions are applied to constrain the free edges, and symmetric boundary conditions are applied to the symmetric surface. We also study the free boundary condition however pull-in at the edge [6,13] does not obvious which is same as experiment.

A thickness of 5.4 mm is employed in UHMWPE under truncate FSP impact model. An initial velocity of 635m/s (experimental ballistic limit velocity) is applied to truncate FSP. The UHMWPE

target plate is modeled by sub-laminate model and each sub-laminate is treated as a combination of several cross-plies. The in-plane element size in central impact region is 0.3 mm and 18 layers is taken in our simulation. The ballistic limit velocity of simulation is 645 m/s and the relative error is 1.6% compared with experiment. The simulated bulge height is 8.1 mm and experimental result is around 10 mm. The element size in central region, FSP and thickness of sub-laminate is chosen to 0.5 mm for other thicknesses (7.5 mm, 10 mm and 15 mm) of UHMWPE.

A series of thicknesses (7.5 mm, 10 mm and 15 mm) of UHMWPE are studied under the impact of cubic FSP. The thickness of each layer is set to 0.5mm and the aspect ratio is chosen to 1. The dimension of central impact zone is 60 mm×30 mm. The element size of cubic FSP is also set to the same value of central impact region in order to avoid stiffness mismatch, as suggested in aforementioned situation. The comparation of experimental and numerical residual velocity under different initial impact velocity are listed in Table 5. We can find that the numerical residual velocity is close to experimental value and the relative error is within 15% except the result about 15 mm thickness.

Table 5: Experimental [21] and numerical residual velocity of UHMWPE under cubic impacting.

Thickness(mm)	Initial velocity(m/s)	Residual velocity (m/s)		Error (%)
		EXP.	NUM.	
7.5	817.2	571.6	547	4.4
7.5	928.7	753	668	11.3
7.5	1079	873.3	819	6.6
7.5	1284.8	1143.2	1005.6	13.7
7.5	1325.8	1164.4	1042	11.7
10	1124.1	827.6	759	9.0
10	1152.2	856.5	787	8.8
10	1155.4	865.7	792	9.3
15	1161.2	666.7	591	12.8
15	1044.1	355.4	442	-19.7

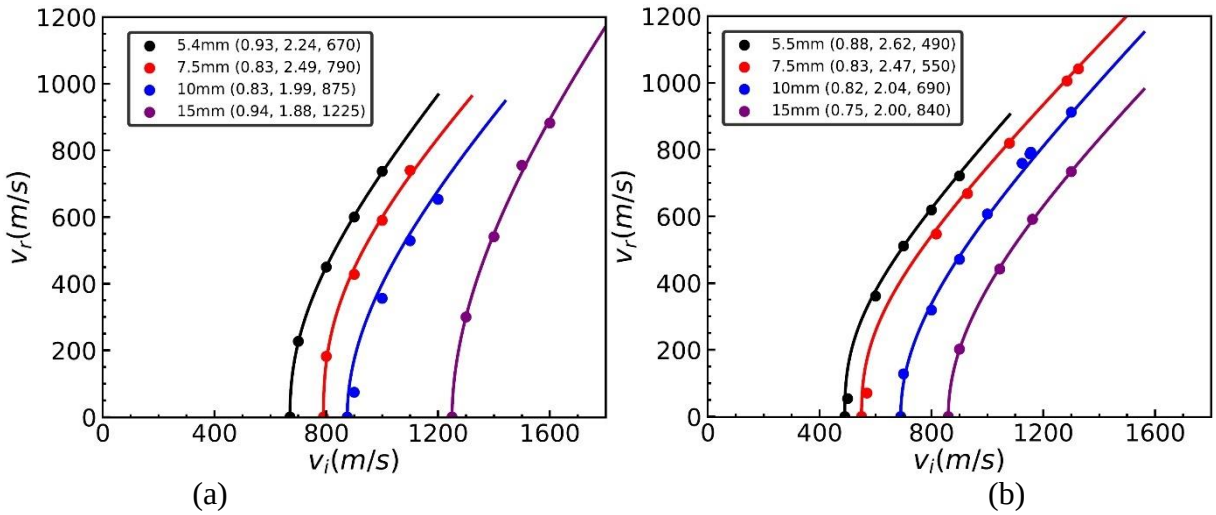

Figure 2: Prediction of numerical residual velocity of projectile about UHMWPE laminate impacted by: (a) truncate FSP, (b) cubic FSP. The numerical results are fitted to Lambert-Jonas equation, the parameters and ballistic limit velocity are given in legend (a, p, v_{bl}).

4. Results and discussion

4.1. Impact process analysis and energy absorption

The relationship between impacted velocity (v_i) and residual velocity (v_r) of projectile can be expressed as Lambert-Jonas [27] equation, which is also known as Recht-Ipson equation. The Lambert-Jonas equation is given as

$$v_r = \begin{cases} 0, v_i < v_{bl} \\ a\left(v_i^p - v_{bl}^p\right)^{1/p}, v_i \geq v_{bl} \end{cases} \tag{8}$$

where a and p are determined from fitting coefficients of v_i and v_r. v_{bl} is ballistic limit velocity. The intersection point of this curve and the abscissa (initial velocity) is the (fitted) ballistic limit velocity. The difference of simulated and fitted ballistic limit velocity is within the range -25~25 m/s. This error is acceptable in ballistic impact. The fitting parameters is very helpful to the analysis of energy balance under ballistic loading condition. The simulation results and Lambert-Jonas fitting curves about truncate and cubic FSPs are shown in Fig. 2. It should be noted that the residual velocity is zero when impacted velocity equals to ballistic limit velocity and the residual velocity will be very large when the impacted velocity is slightly larger than ballistic limit velocity.

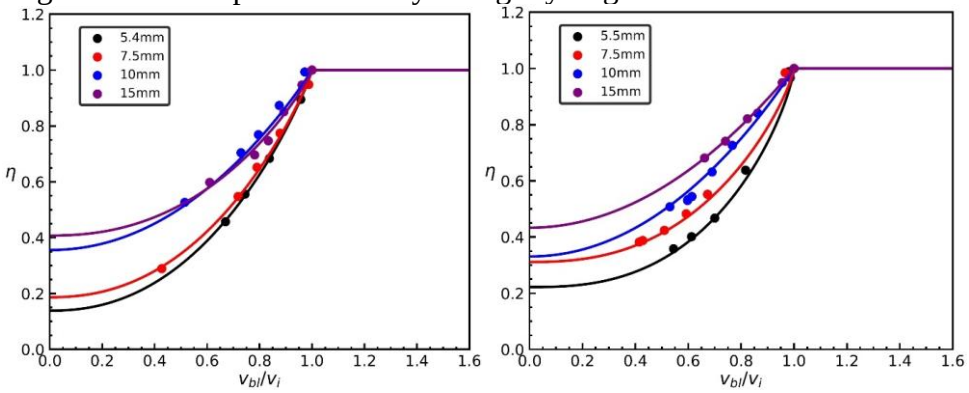

(a) (b)

Figure 3: Energy absorption rate about UHMWPE laminate impacted by: (a) truncate FSP, (b) cubic FSP.

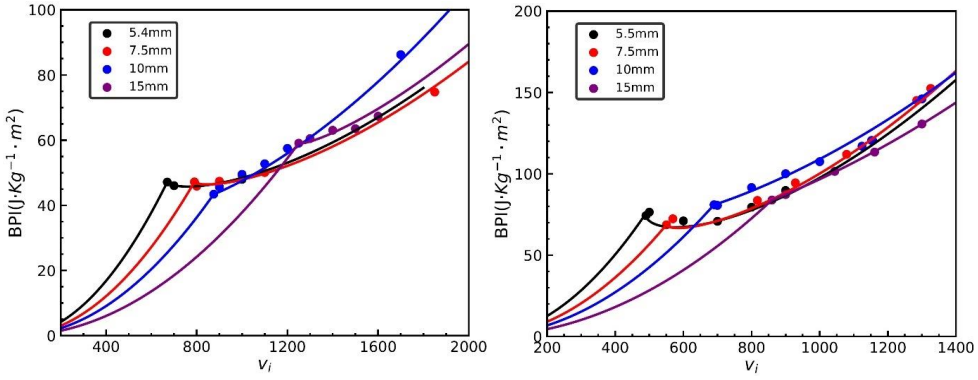

(a) (b)

Figure 4: Ballistic performance index (BPI) about UHMWPE laminate impacted by: (a) truncate FSP, (b) cubic FSP.

The kinetic energy dissipation of projectile is assumed to equal to the energy absorption of composite laminate. E_a is calculated by the difference of kinetic energy before and after the projectile penetrating the target laminate and it is given by

$$E_a = \frac{1}{2} m_p \left(v_i^2 - v_r^2 \right) \tag{9}$$

where m_p, v_i and v_r are mass of impacted projectile, impacted velocity and residual velocity of projectile. The energy absorption rate η is defined by

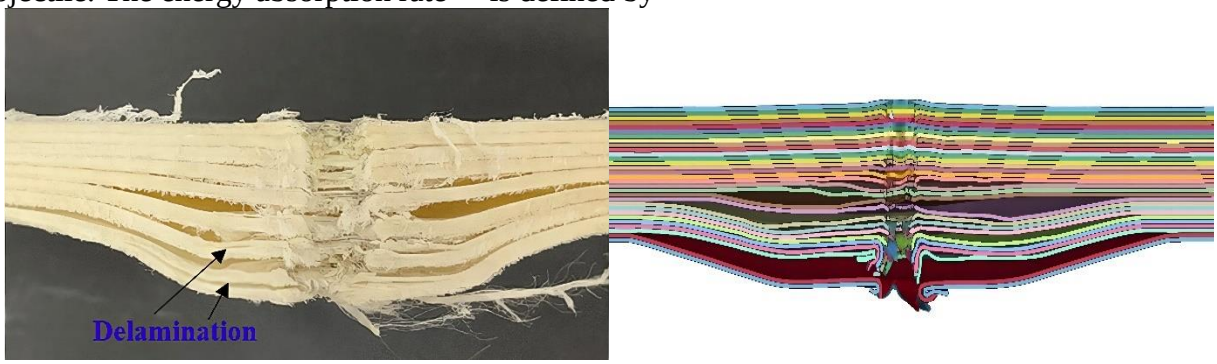

(a) (b)

Figure 5: Comparison between experiment and numerical simulation result: (a) experiment [6], (b) simulation.

$$\eta = \frac{E_a}{E_i} = \frac{E_a}{\frac{1}{2} m_p v_i^2} = 1 - \left(\frac{v_r}{v_i} \right)^2 \tag{10}$$

where E_i is impact energy or initial energy and it is the initial kinetic energy of projectile. The absorption energy is increased with impacted energy impacted by truncate and cubic FSPs when impact velocity is greater than ballistic limit velocity. After substituting Eq. (8) to Eq. (10), energy absorption rate can be written in following equation:

$$\eta = 1 - a^2 \left(1 - \frac{v_{bl}^p}{v_i^p} \right)^{2/p}, v_i \geq v_{bl} \tag{11}$$

The energy absorption rate η equals to one when $v_i < v_{bl}$ since the residual velocity is zero. In this case, all of the energy is absorbed by target laminate. The energy absorption rate about UHMWPE laminate impacted by truncate and cubic FSPs in terms of a non-dimensional velocity $v_{bl} < v_i$ is given in Fig. 3. It should be noted that the larger the thickness of target the greater the energy absorption rate under same non-dimensional velocity. A larger non-dimensional velocity is needed for thin composite in order to obtain a same energy absorption rate compared with larger thickness target. It means that large the energy absorption rate can be obtained when v_i closes to ballistic limit velocity v_{bl}. Ballistic performance index (BPI), an indicator that evaluates both weight and protection capacity, is used to characterize the ballistic performance of laminate. It is calculated as follows:

$$BPI = \frac{E_a}{\rho_A} \tag{12}$$

where ρ_A are areal density of target laminate. After substituting Eqs. (8) and (9) to Eq. (12), BPI can be rewritten in

$$BPI = \frac{\frac{1}{2}m_p}{\rho_A}\left[v_i^2 - a^2\left(v_i^p - v_{bl}^p\right)^{2/p}\right], v_i \geq v_{bl} \tag{13}$$

The *BPI* in terms of impacted velocity under impacted by truncate and cubic FSPs is given in Fig. 4. When the velocity is smaller than ballistic limit velocity of 5.4 mm (5.5 mm for cubic FSP impacting) laminate, the protection capacity of composite per areal density decreases with composite thickness. The resistance capacity is almost same about 5.4 mm (5.5 mm impacted by cubic FSP) and 7.5 mm thick UHMWPE when the impacted velocity is large enough. The protection capacity of 10 mm thickness is the best of 4 different thicknesses for velocity is larger than ballistic limit velocity of 10 mm thickness laminate.

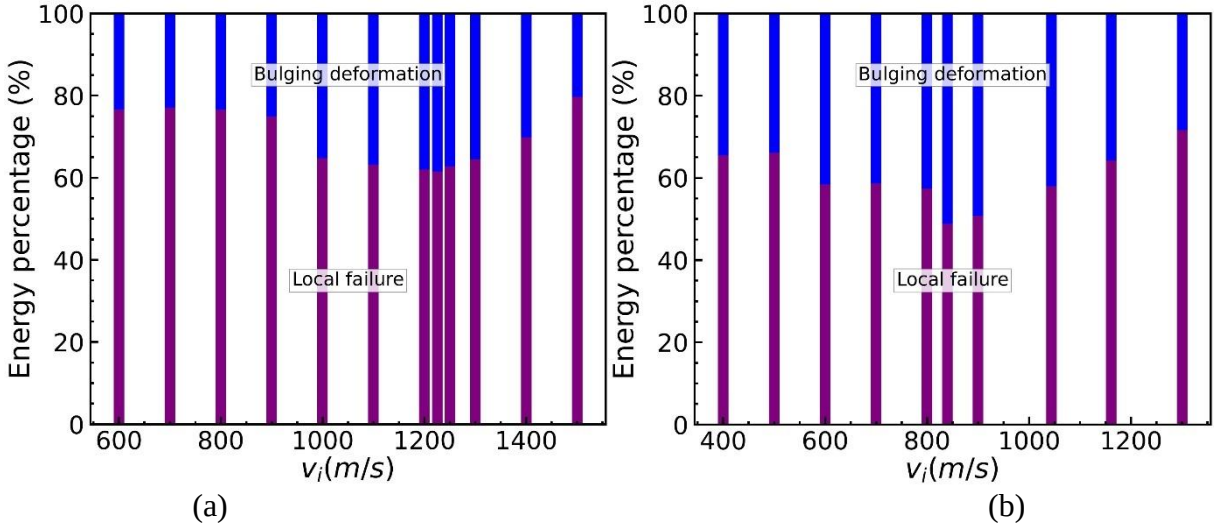

Figure 6: Energy fraction of local failure and bulging deformation stages of 15 mm thick UHMWPE laminate impacted by: (a) truncate FSP, (b) cubic FSP at selected initial impacted velocity.

4.2. Penetration mechanism

The process of projectile penetration can be divided in two sequential stages of local failure and bulging deformation [12]. Extensive delamination failure is observed during experiments and simulations [6]. Delamination is observed in bulge deformation stage, however no or little delamination is observed during local failure stage in our numerical result. Local failure is also known as shear plugging. Bulge deformation is out-of plane deflection and the predominant failure is fiber tension. The difference in failure model can also be observed from scanning electron microscope (SEM) results and it is significant in two stages. The fiber fracture surface is clean and flat in local failure or shear plugging, while fiber failing in bulging deformation or fiber tension undergo significant elongation and reduction in diameter [10]. A large amount of elastic recoil of the fibers at the penetration site is observed in high-speed video [10] which is also exhibited in our numerical result (see Fig. 5). Fiber-matrix debonding could not be modeled by macro-scale simulation (e.g. finite element analysis with sub-laminate model).

The local failure and bulging deformation stages are also observed during the simulation of penetration process for thin laminate (e.g. 5.4mm) in our work, however only bulging or tensile failure is displayed for thin laminate (less than 10 mm thick) in [10]. In this case, it can be derived that both failure stages will be observed in composite laminate regardless of the thickness. Local failure stage is dominant in the two stages in our work and it is consistent with the thick composite laminate [10], however it is opposite in others result [12]. Energy fraction of local failure and bulging deformation stages of 15 mm thick UHMWPE is listed in Fig. 6. The energy fraction of bulging deformation keeps constant at the beginning and then it increases with impacted velocity. Finally, it decreases with impacted velocity. The maximum value of energy fraction about bulging deformation is at ballistic limit velocity. This trend of energy fraction is similar to the result in [12]. There is a jump of energy absorbed in bulge deformation stage impacted by cubic FSP, however this phenomenon does not exist for truncate FSP. The corresponded situation may be related to to the shape of projectile. The amount of bulging deformation energy fraction about cubic FSP is larger than the value about truncate FSP. The reason is that the cubic FSP has a large mass and this makes the interval of local failure become short. In this case, the transition velocity of these two stages impacted by cubic FSP is larger than the velocity in truncate FSP. The deformation of FSP can be ignored due to the deformation is very small for bulging failure stage. The projectile is mainly deformed for the local failure stage. As the impact velocity of the fragment increasing, the shape of the FSP begins to change into mushrooming.

5. Conclusions

A 3D continuum finite element with sub-laminate composite model is proposed to simulate ballistic impact performance of UHMWPE composite laminate. Target composites under different impacted velocities and thicknesses are investigated. The main conclusions are summarized as follows:

(1) The residual velocity can be fitted in terms of impacted velocity through Lambert-Jonas equation. The absorption energy increases with impacted velocity of projectile when the velocity is larger than ballistic limit velocity. The energy absorption rate increases with composite thickness when the non-dimensional velocity keeps constant. The result of BPI shows that the protection capacity of 10 mm thick composite laminate is best.

(2) The failure of composite laminate can be divided in two stages: local failure stage and bulging deformation stage. The energy fraction of two stages is dominated by local failure stage. The energy fraction of bulging deformation stage increases with impacted velocity and then decreases with the velocity, and the maximum value of the energy fraction is obtained when the velocity reaches ballistic limit velocity. The energy absorption mechanism may be related to the shape of projectile. The dominant failure stage also depends on the specific composite materials.

Acknowledgements

This work is funded by AECC Aegis Advanced Protective Technology Co., Ltd under grant YF240701.

References

[1] van der Werff H., Heisserer U. (2016) High-performance ballistic fibers: ultra-high molecular weight polyethylene (UHMWPE), in: Advanced fibrous composite materials for ballistic protection, Elsevier, pp. 71–107.
[2] He Y., Jiao Y., Zhou J.Q., Lei H., Jia N., Chen L., Zhang D. (2022) Ballistic response of ultra-high molecular weight polyethylene laminate impacted by mild steel core projectiles, International Journal of Impact Engineering 169, 104338.
[3] Sapozhnikov S., Kudryavtsev O., Zhikharev M. (2015) Fragment ballistic performance of homogenous and hybrid

thermoplastic composites, International Journal of Impact Engineering 81, 8–16.
[4] Cline J., Love B. (2020) The effect of in-plane shear properties on the ballistic performance of polyethylene composites, International Journal of Impact Engineering 143, 103592.
[5] Zhang R., Qiang L.-S., Han B., Zhao Z.-Y., Zhang Q.-C., Ni C.-Y., Lu T.J. (2020) Ballistic performance of UHMWPE laminated plates and UHMWPE encapsulated aluminum structures: Numerical simulation, Composite Structures 252, 112686.
[6] Zhang R., Han B., Zhong J.-Y., Qiang L.-S., Ni C.-Y., Zhang Q., Zhang Q.-C., Li B.-C., Lu T.J. (2022) Enhanced ballistic resistance of multilayered cross-ply UHMWPE laminated plates, International Journal of Impact Engineering 159, 104035.
[7] Zhao C.-Z., Qiang L.-S., Zhang R., Zhang Q.-C., Zhong J.Y., Zhao Z.-Y., Lu T.J. (2023) Dynamic response of uhmwpe plates under combined shock and fragment loading, Defence Technology 27, 9–23.
[8] He Y., Jiao Y., Zhou J.Q., Zhang D., Lei H., Chen L. (2023) Influence of projectile physical state on ballistic energy absorption capacity of uhmwpe laminate: Experiment and simulation, Composite Structures 326, 117607.
[9] Segala D., Cavallaro P. (2014) Numerical investigation of energy absorption mechanisms in unidirectional composites subjected to dynamic loading events, Computational Materials Science 81, 303–312.
[10] Nguyen L.H., Ryan S., Cimpoeru S.J., Mouritz A.P., Orifici A.C. (2015) The effect of target thickness on the ballistic performance of ultra high molecular weight polyethylene composite, International Journal of Impact Engineering 75, 174–183.
[11] Yang S., Yan Z., Gao Y., Zhang Y., Wang Y., Liu Z. (2023) Numerical and theoretical modeling of the elastic-plastic bulging deformation of uhmwpe composite laminate under high-speed impact, International Journal of Impact Engineering 182, 104771.
[12] Zhang R., Han B., Zhou Y., Qiang L.-S., Zhao C.-Z., Zhao Z.-Y., Zhang Q.-C., Ju Y.-Y., Lu T.J. (2023) Mechanism-driven analytical modelling of uhmwpe laminates under ballistic impact, International Journal of Mechanical Sciences 245, 108132.
[13] Nguyen L. H., Lässig T. R., Ryan s., Riedel W., Mouritz A.P., Orifici A.C. (2016) A methodology for hydrocode analysis of ultra-high molecular weight polyethylene composite under ballistic impact, Composites Part A: Applied Science and Manufacturing 84, 224–235.
[14] Hazzard M. K., Trask R. S., Heisserer U., Van Der Kamp M., Hallett S. R. (2018) Finite element modelling of dyneema® composites: from quasi-static rates to ballistic impact, Composites Part A: Applied Science and Manufacturing 115, 31–45.
[15] Johnson G.R., Cook W. H. (1983) A constitutive model and data for metals subjected to large strains high strain rates and high temperatures, in: Proc. of 7th Int. Symp on Ballistics, The Hague.
[16] Johnson G.R., Cook W. H. (1985) Fracture characteristics of three metals subjected to various strains, strain rates, temperatures and pressures, Engineering fracture mechanics 21 (1), 31–48.
[17] Chen G., Chen Z.F., Xu W.F., Chen Y.M., Huang X.C. (2007) Investigation on the J-C ductile fracture parameters of 45 steel (in chinese), Explosion & Shock Waves.
[18] Steinberg D. (1991) Equation of state and strength properties of selected materials, Tech. rep., Lawrence Livermore National Laboratory.
[19] Mohd Nor M., Ho C., Ma'at N., Kamarulzaman M. (2020) Modelling shock waves in composite materials using generalised orthotropic pressure, Continuum mechanics and thermodynamics 32, 1217–1229.
[20] Guo B., Ren K., Li Z., Chen R. (2021) Modelling on shock-induced energy release behavior of reactive materials considering mechanical-thermal-chemical coupled effect, Shock and Vibration 2021, 1–12.
[21] Hu N., Zhu X., Hou H., Chen C. (2014) Estimating method for the ballistic limit of ultra-high molecular weight polyethylene fiber-reinforced laminates under high-velocity fragment penetration (in chinese), Chinese Journal of Ship Research 9 (4), 55–62.
[22] Li J., Liu M. (2022) An analytical model to predict the impact of a bullet on ultra-high molecular weight polyethylene composite laminates, Composite Structures 282, 115064.
[23] Dogan F., Hadavinia H., Donchev T., Bhonge P.S. (2012) Delamination of impacted composite structures by cohesive zone interface elements and tiebreak contact, Central European Journal of Engineering 2, 612–626.
[24] Lässig T., Bagusat F., Pfändler S., Gulde M., Heunoske D., Osterholz J., Stein W., Nahme H., May M. (2017) Investigations on the spall and delamination behavior of UHMWPE composites, Composite Structures 182, 590–597.
[25] Karthikeyan K., Russell B., Fleck N., Wadley H. (2013) Deshpande, The effect of shear strength on the ballistic response of laminated composite plates, European Journal of Mechanics-A/Solids 42, 35–53.
[26] Staniszewski J.M., Boyd S.E., Bogetti T.A. (2022) A multi-scale modeling approach for UHMWPE composite laminates with application to low-velocity impact loading, International Journal of Impact Engineering 159, 104031.
[27] Lambert J., Jonas G. (1852) Towards standardization in terminal ballistics testing: velocity representation, USA Ballistic Research Laboratories, Aberdeen Proving Ground, MD, Technical Report.